# Evidence for decreased precipitation variability in the Yucatán Peninsula during the mid-Holocene

Serrato Marks, Gabriela[a,b*], Medina-Elizalde, Martín[c], Burns, Stephen[d], Weldeab, Syee[e], Lases-Hernandez, Fernanda[f], Cazares, Gabriela[a], McGee, David[a]

[a] Department of Earth, Atmospheric, and Planetary Sciences (EAPS), Massachusetts Institute of Technology, Cambridge, MA, USA
[b] Marine Geology and Geophysics Department, Woods Hole Oceanographic Institution, Woods Hole, MA, USA
c Department of Geosciences, Auburn University, AL, USA
d Department of Geosciences, University of Massachusetts Amherst, Amherst, MA, USA
e Department of Earth Science, University of California, Santa Barbara, CA, USA
f Centro de Geociencias, UNAM Campus Juriquilla, Querétaro, Mexico.

*Corresponding Author. gserrato@mit.edu

**Abstract**
The Yucatán Peninsula has a complex hydroclimate with many proposed drivers of interannual and longer-term variability, ranging from coupled ocean-atmosphere processes to frequency of tropical cyclones. The mid-Holocene, thought to have had warmer north Atlantic sea surface temperatures, provides an interesting opportunity to test the relationship between Yucatán Peninsula precipitation and ocean temperature. Here we present a new, ~annually resolved speleothem record of stable isotope ($\delta^{18}O$ and $\delta^{13}C$) and trace element (Mg/Ca and Sr/Ca) ratios for a section of the mid-Holocene (5.2-5.7 kyr BP). A meter-long stalagmite from Río Secreto, a cave system in Playa del Carmen, Mexico, was dated using U-Th geochronology and layer counting, yielding ~decadal age uncertainty. The new proxy data were compared to a previously published late Holocene stalagmite from the same cave system, allowing us to examine changes in hydrology over time without potential inter-cave differences. The $\delta^{18}O$, $\delta^{13}C$ and trace element data consistently indicate higher mean precipitation and lower precipitation variability during the mid-Holocene compared to the late Holocene. Despite this reduced variability, spectral analysis suggests that multi-decadal precipitation variations were persistent in regional hydroclimate during the mid- and late Holocene. Wet-dry oscillations occurred in association with the higher summer solar input and higher mean precipitation of the mid-Holocene, though with reduced amplitude compared to the late Holocene. We therefore conclude that the Yucatán Peninsula is susceptible to dry periods across climate mean states.

Keywords: Yucatán Peninsula, speleothems, hydroclimate, trace elements, oxygen isotopes, carbon isotopes, drought.

Key points:

- Stable isotope data show a wetter, less variable mid-Holocene climate in the Yucatan Peninsula compared to the late Holocene
- Single cave, multi-stalagmite analyses are effective ways to examine hydroclimate variability over time
- Speleothem Mg/Ca and Sr/Ca ratios have potential for use as climate proxies in the Yucatán Peninsula

## 1 Introduction

The Yucatán Peninsula (YP) harbors diverse ecosystems, including the Mesoamerican barrier reef and tropical rainforests, and has been inhabited by Maya societies for thousands of years. Biological systems and human societies in the region developed under limited surface and groundwater availability and have therefore been vulnerable to hydroclimate extremes. There has been extensive research on the potential drivers of YP climate variability during the Common Era, 2,000 years before present (yr BP) to present, and on the role of drought in the decline of Maya civilization during the Preclassic (~180 and 240 CE) and Terminal Classic Periods (750-950 CE) (*e.g.* Hodell et al., 1995, Curtis et al., 1996, Medina-Elizalde et al., 2010, Medina-Elizalde et al., 2016a).

Climate simulations and paleoclimate records suggest that late Holocene precipitation in the YP was linked to North Atlantic climate variability. Potential controls include changes in sea surface temperature (SST), sea level pressure (SLP) (Bhattacharya et al., 2017), tropical cyclone variability (Frappier et al., 2007, 2014; Medina-Elizalde et al., 2016a), and the mean position of the Intertropical Convergence Zone (ITCZ)(*e.g.* Bush et al., 2009; Lechleitner et al., 2017; Ridley et al., 2015; Pollock et al., 2016). These climate variations are likely linked, further complicating diagnostics (McGee et al., 2014). YP precipitation variability also suggests a link with El Niño-Southern Oscillation (ENSO) in the Pacific (Frappier et al., 2014; Giannini et al., 2000, Lachniet et al., 2017; Medina-Elizalde et al., 2016a, 2016b, 2017; Metcalfe et al., 2009; Pollock et al., 2016; Stahle et al., 2012).

However, the majority of the paleoclimate records from the YP are confined to the late Holocene, and do not extend into the mid- or early Holocene. The mid-Holocene is of particular interest to investigate the role of external forcing on hydroclimate variability in the Caribbean region. During the mid-Holocene, solar radiation was higher in the Northern hemisphere (NH) during the boreal summer relative to the late Holocene and present (Hoddell et al., 1995; Laskar et al., 2004) and ENSO variability was markedly decreased (Carré et al., 2014; Chen et al., 2016; Emile-Geay et al., 2016). Increased NH summer radiation produced stronger seasonality and favored higher summer SSTs in the North Atlantic and Caribbean, as suggested by previous studies (Marcott et al., 2013; Marsicek et al., 2018). Specifically, a proxy compilation showed that North Atlantic (30˚N to 90˚N) SSTs cooled by $2^{o}$C from 7 kyr BP to 100 yr BP (Marcott et al., 2013). Based upon modern connections between the North Atlantic and Caribbean hydroclimate (*e.g.* Bhattacharya et al., 2017) we expect that the mid-Holocene was wetter and less variable in precipitation than the late Holocene or the present.

The existing paleoclimate records in the YP are based on proxy data from various archives, including cave speleothems (*e.g.* Akers et al., 2016; Frappier et al., 2014; Pollock et al., 2016) and lake, sinkhole, wetland, and swamp sediment cores (Curtis et al., 1996; Douglas et al., 2015; Guttierez-Ayala et al., 2012; Hodell et al., 2005; Metcalfe et al., 2009; Rosenmeier et al., 2002; Roy et al., 2017). Interpretations of these paleoclimate records do not offer a consensus regarding the magnitude and frequency of precipitation variability and underlying drivers during the Holocene. Discrepancies among available paleoclimate records do not indicate that these records are erroneous; instead, they likely reflect climatological differences among locations, chronological uncertainties, differences in the temporal resolution, and the complexity inherent in using geochemical proxies to infer past climates. With few exceptions (Kennett et al., 2012; Medina-Elizalde et al., 2010, Richey et al., 2015, Ridley et al., 2015), most available paleoclimate records do not have enough temporal resolution to investigate interannual to decadal hydroclimate variability in the region, and most high-resolution studies are limited to the Late Holocene. Finally, no existing studies on stalagmite geochemical records from the YP have compared multiple stalagmite specimens from the same cave. Therefore, there is a need for climate archives that come from the same location, use the same proxies, and have high temporal resolution to investigate changes in climate variability through the Holocene.

In order to refine our understanding of hydroclimate variability in the YP and its underlying drivers during the mid-Holocene, we present stalagmite $\delta^{18}O$, $\delta^{13}C$, Mg/Ca and Sr/Ca records spanning the interval between 5.2 and 5.7 kyr before present (BP). The stalagmite we use, named Yáax (which means "first" in Yucatec Mayan), was collected in April 2013 from an isolated chamber in the Rio Secreto Cave system, located in the northeastern YP. An extensive drip water monitoring system was installed in 2014; Yáax was sampled closest to Drip Station A referenced in Lases-Hernandez et al. (2019). Yáax is a ~1 m tall calcite stalagmite, which was partially collapsed at the time of collection. It presents visually distinct lamination, allowing development of an age model based on laminae counting and U-series dating (see Methods). Stalagmite $\delta^{18}O$ and $\delta^{13}C$ have often been used to infer changes in precipitation in this region (*e.g.* Medina-Elizalde et al., 2010; Ridley et al., 2015; Pollock et al., 2016), while Mg/Ca and Sr/Ca have not been examined previously in the YP, but have been interpreted to reflect precipitation amount in other settings.

This study examines the new stalagmite record in comparison to another stalagmite-based precipitation record, known as Itzamna, from the same well-studied cave, spanning ~3 to 1.6 kyr BP (Medina-Elizalde et al., 2016a). Stalagmite proxy records from the same location allow us to contrast inferred mid- and late Holocene hydroclimate variability, and minimize the uncertainty associated with comparing stalagmite proxy records from different locations and cave environments.

### *1.2 Regional climate*

The YP experiences a strong seasonality in precipitation amount (Figure 1). The rainy season occurs in the summer, often interrupted by decreased rainfall in July or August (Karmalkar et al., 2011; Lases-Hernandez et al., 2019; Muñoz et al., 2008). About 70% of annual rainfall occurs between June and November (Medina-Elizalde et al., 2016b; Figure 1). Maximum precipitation often occurs in September, when the ITCZ is at its northernmost position and Atlantic tropical cyclone frequency peaks (Kovacs et al., 2017; Lases-Hernandez et al., 2019). Strong easterly winds, known as the Caribbean Low Level Jet (CLLJ), bring moisture from the warm Caribbean Sea to the YP (Muñoz et al., 2008); if enhanced, the CLLJ drives increased moisture transport and convergence in the region (Karmalkar et al., 2011; Mestas-Nuñez et al., 2007; Muñoz et al., 2008;). The large-scale structure of the vertically-integrated water vapor fluxes associated with the CLLJ links the Caribbean and Gulf of Mexico regions to climate regimes in the US, particularly during boreal summer (Mestas-Nuñez et al., 2007; Muñoz et al., 2008). We note that historical precipitation variability in the YP region is linked to that of the broader Caribbean region, particularly the northern sector, as indicated by spatial-temporal correlation analyses of instrumental precipitation records (*e.g.* Medina-Elizalde et al., 2017).

*1.3 Climate proxies*

Stalagmite $\delta^{18}O$ records in Mesoamerica, including the YP, are interpreted to reflect changes in precipitation amount (*e.g.* Akers et al., 2016; Lachniet et al., 2017; Medina-Elizalde et al., 2016a, 2016b), with more negative $\delta^{18}O$ values indicating increased precipitation, as expected from an amount effect, or the empirical relationship between precipitation amount and $\delta^{18}O$ composition observed in the tropics from seasonal to interannual timescales (Burns et al., 1998; Dansgaard, 1964; Lases-Hernandez et al., 2019; Vuille et al., 2003). Changes in $\delta^{13}C$ in stalagmites reflect a number of local processes associated with the soil cover, epikarst and vadose zone (Genty et al., 2006). Some of the most common controls include the ratio of C3 to C4 vegetation above the cave (Burns et al., 2016; Dorale et al., 1998; Webb et al., 2004;) and the amount of degassing in the vadose zone (Lachniet et al., 2004). Rainfall amount can influence drip water $\delta^{13}C$ (and therefore stalagmite $\delta^{13}C$) by affecting soil moisture and organic matter production, bedrock dissolution, degassing, and prior calcite precipitation (PCP) (Genty et al., 2006; Ridley et al., 2015; Wong and Breecker, 2015).

In low-latitude caves where the overlying vegetation is expected to remain relatively stable over time, stalagmite $\delta^{13}C$ variability can reflect precipitation amount, as observed in Belize (Ridley et al., 2015). Low precipitation enhances PCP, increases bedrock carbon contributions and decreases soil bio-productivity, all ultimately increasing drip water $\delta^{13}C$ and stalagmite $\delta^{13}C$ (*e.g.* Ridley et al., 2015; Pollock et al., 2016). In the YP, where the type of vegetation is also expected to have remained relatively constant, particularly during the mid-Holocene before extensive human activity, stalagmite $\delta^{13}C$ could reflect precipitation amount.

Although stalagmite $\delta^{18}O$ and $\delta^{13}C$ records have been widely interpreted as hydroclimate proxies, they are not without complexities. Stalagmite $\delta^{18}O$ can be influenced by changes in moisture source and upstream water vapor history. Similarly, stalagmite $\delta^{13}C$ can be impacted by soil and karst processes not directly related to precipitation variability (Hellstrom et al., 1998, Genty et al., 2001). Moreover, both $\delta^{18}O$ and $\delta^{13}C$ can also be affected by kinetic fractionation, especially in low humidity environments. Despite these potentially complicating issues, previous studies in the YP and Belize present multiple lines of evidence that stalagmite $\delta^{18}O$ and $\delta^{13}C$ can record local and regional precipitation amount (Medina-Elizalde et al., 2010, 2016a, 2016b, 2017; Ridley et al., 2015; Pollock et al., 2016). We analyze Mg/Ca and Sr/Ca ratios to examine their magnitude and frequency variability and to test interpretations from the more conventional $\delta^{18}O$ and $\delta^{13}C$ records. This is the first study that examines Mg/Ca and Sr/Ca ratios in a stalagmite from the YP region.

Several stalagmite analyses in other locations have applied Mg/Ca and Sr/Ca for hydroclimate reconstruction (*e.g.* Roberts et al., 1998; Fairchild et al., 2001; Cruz et al. 2017; Lewis et al., 2011; Steponaitis et al., 2015). Trace element to calcium ratios can track PCP and/or water-rock interactions, which change based upon soil and water conditions in the local environment (*e.g.* Fairchild et al., 2000, 2001; Cruz et al., 2017; Sinclair et al., 2012). In drier conditions, water moves more slowly through the karst above a cave, so it has more time to degas and become saturated with calcite (Tremaine and Froelich, 2013). During PCP, Mg and Sr are preferentially excluded from the calcite crystal lattice, so Mg/Ca and Sr/Ca ratios in groundwater increase with PCP (Fairchild et al., 2000). Non-PCP interactions between water and host rock, also referred to as calcite recrystallization, can also occur in the karst, especially when water residence time is high during dry periods. The chemical signature of recrystallization is similar to that of PCP, but with a different relationship between Mg/Ca and Sr/Ca (Sinclair et al., 2012). Therefore, Mg/Ca and Sr/Ca in stalagmites provide an estimate of aquifer recharge and water availability that can serve as an independent proxy, and provide a method to examine whether stalagmite $\delta^{18}O$ primarily reflects changes in local moisture availability (Tremaine & Froelich, 2013).

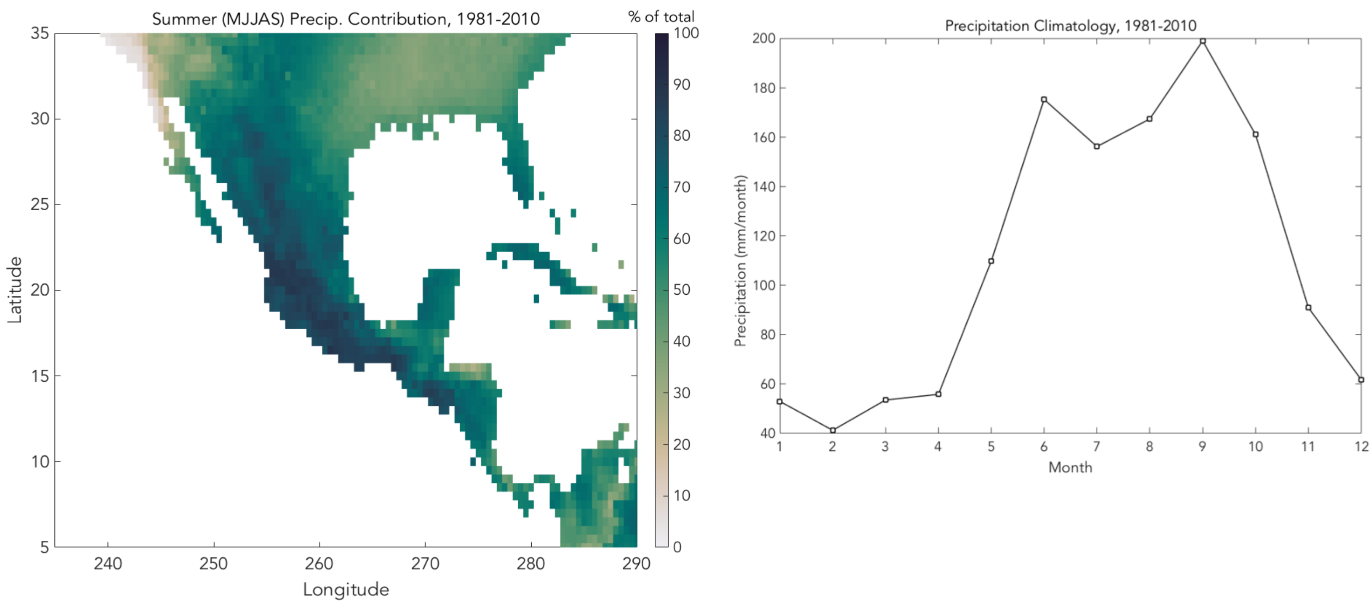


*Figure 1. Seasonality of precipitation at the Yucatan Peninsula and surrounding area; all rainfall data are from the University of Delaware Terrestrial Air Temperature and Precipitation dataset (Willmott & Matsuura, 2001). Left: Percentage of total rainfall from the summer (MJJAS), pink circle indicates the location of Río Secreto Cave, our study site. Right: monthly precipitation closest to Rio Secreto.*

## 2 Methods

*2.1 Regional setting and cave system*

We collected the stalagmite outside the city of Playa del Carmen, in the northeast YP (20°35.244'N, 87°8.042'W, 10-20m above sea level). The Rio Secreto Cave (RS) entrance is about 5 km from the Caribbean coast; therefore, the locale has a strong maritime influence from the Caribbean.

Temperature and relative humidity in RS have been monitored continuously since 2014. Annual mean temperature in the collection chamber varied by 0.1˚C, from 24.6 to 24.7˚C (Medina-Elizalde et al., 2016b; Lases-Hernandez et al., 2019). The steady temperature limits the effect of calcification temperature on stalagmite $\delta^{18}O$ (hereafter $\delta^{18}O_{calcite}$). RS has a relative humidity of 99.6 ± 0.9% throughout the year (Medina-Elizalde et al., 2016b; Lases-Hernandez et al., 2019).

Three years of drip water $\delta^{18}O$ ($\delta^{18}O_{drip}$) monitoring at 16 drip sites indicate that $\delta^{18}O_{drip}$ reflects the $\delta^{18}O$ composition of precipitation ($\delta^{18}O_{precip}$), and that evaporation does not influence $\delta^{18}O_{drip}$. The average $\delta^{18}O_{drip}$ is -3.9 ± 0.2‰ (± 2*standard error, hereafter 2SE; n = 1043 drip samples collected over 3 years), and the amount-weighted $\delta^{18}O_{precip}$ is -3.7 ± 0.5‰ (n = 36 monthly rainfall samples; arithmetic mean $\delta^{18}O_{precip}$ = -2.6 ± 0.5‰; ± 2SE)(Lases-Hernandez et al., 2019). Therefore, the cave drip water accurately records regional $\delta^{18}O_{precip}$ within error. Rainfall infiltration rates vary, with some drip sites showing increased discharge immediately after rainfall events and others lagging by weeks to three months (Lases-Hernandez et al., 2019).

Drip water samples closest to the Yáax collection site show muted ~2‰ intra-annual (seasonal) variability in $\delta^{18}O$ (Lases-Hernandez et al., 2019), and annual mean $\delta^{18}O_{drip}$ similar to the amount-weighted annual mean $\delta^{18}O_{precip}$, which suggests that this chamber has a large reservoir with a mixture of seasonal and seepage flow that averages approximately one year of rainfall accumulation (Lases-Hernandez et al., 2019). Therefore, this study focuses on variability at annual or greater scales. The stalagmite was sampled for proxies with the aim of producing ~annual resolution data.

*2.3 U-Th dating, age modeling and microstratigraphy*

The age model for Yáax is constrained by U-Th dating of 15 horizons distributed throughout the length of the stalagmite, performed at MIT (Figure 2). Analyses included replicates (Figure 2). Dating samples weighing ~150 mg were drilled with a vertical mill. Powders were dissolved and spiked with a $^{229}Th$–$^{233}U$–$^{236}U$ tracer. Based on methods detailed in Edwards et al. (1987), U and Th were isolated using co-precipitation with Fe oxyhydroxides, and eluted using columns with AG1-X8 resin. A total procedural blank was included with each set of dating samples. U and Th fractions were measured on a Nu Plasma II-ES MC-ICP-MS, as described in Burns et al. (2016). We used an initial $^{230}Th/^{232}Th$ value of 4.4 ± 2.2 for detrital correction.

Five of the 15 total dates were not included in the final age model due to low reproducibility, location outside hiatuses, or proximity to possible dissolution features (Supplemental Information). Replicates from the same depth were discarded if they did not overlap within 2SD, and samples within 10 mm of a possible dissolution feature were not included.

Age-depth relationships were calculated with the COPRA program (Breitenbach et al., 2012) in MATLAB (version R2018b). The age-depth model was based on 2000 Monte Carlo simulations of 10 U-Th dates. The median age model was selected instead of the mean to reduce the risk of extreme models having an outsized impact on the final age model. We calculated upper and lower bounds of the 95% CI, but we are only using the median age-depth model for our analysis. The median age model and the 95% CI limits all fall within the 2SD uncertainty of each U-Th date.

Age modeling results showed that the stalagmite spans 528 ± 76 years and visual counts of the same vertical extent yielded 482 ± 38 layers (mean ± 2SD of multiple counts by GSM and GC). The U-Th age and layer count overlap within uncertainty, so we established a layer count-enabled age-depth model. We used two U-Th dates (one from the top and one from the bottom) as markers of absolute age, then used layer counts between other U-Th data points to measure relative change in age. We used the date second from the bottom as an anchor (instead of the date closest to the bottom) because of the potential shift in growth rate observed from age-depth modeling. With this method, we generated a simplified age-depth model based on a cubic function ($r^2 > 0.99$; Figure 2) which is used to calculate ages for the time series of geochemical proxies.

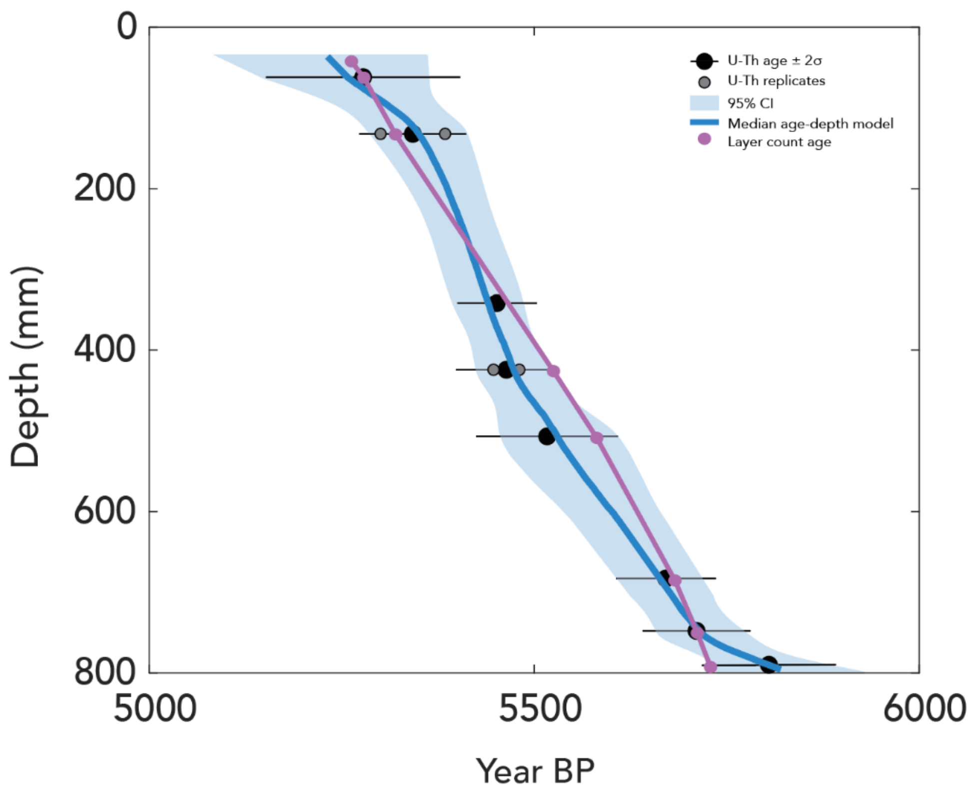


*Figure 2. Age-depth relationship for Yáax based on Monte Carlo modeling of ten U-Th dating horizons and layer counting. The median and 95% confidence interval age models used U-Th dates only; the layer count-enabled model is shown in purple, and is used for the time series plots in subsequent figures.*

Yáax shows a high deposition rate with visually distinct ~2 mm-thick layers throughout the stalagmite, likely reflecting annual deposition (Figure 2). The layers were distinct enough to count and measure in photographs or hand sample, allowing for counting without microscopy or thin sections.

At the bottom of the stalagmite (794 mm from the top), there is a ~50 mm-long, relatively dark region that looks more similar to the outer crust than to the rest of the stalagmite (Figure 3C). There are no visible layers within the region, suggesting that the layering was dissolved and recrystallized with newer crust. XRD analysis showed that this region is calcite with added silica (Supplementary Information). Qualitatively, this region is denser and harder, consistent with the presence of minerals harder than calcite. Yáax was found partially collapsed, so we infer that this dark area is a diagenetically altered segment. Both the dark region and the layers below were not included in this study.

Visual inspection revealed a potential hiatus near the top of the sample (Figure 3D), visible as a color change in the calcite and a 2 mm-thick brown layer. Therefore, the region above the deposited dark material (top – 23 mm from top) was not used in climate analysis or age-depth calculations. After these regions were excluded, the useable region of Yáax spans 455 ± 38 years (5720 to 5266 yr BP; 2SD uncertainty based on layer counting). This age is still within 2SD uncertainty of the original age model without layer counting.

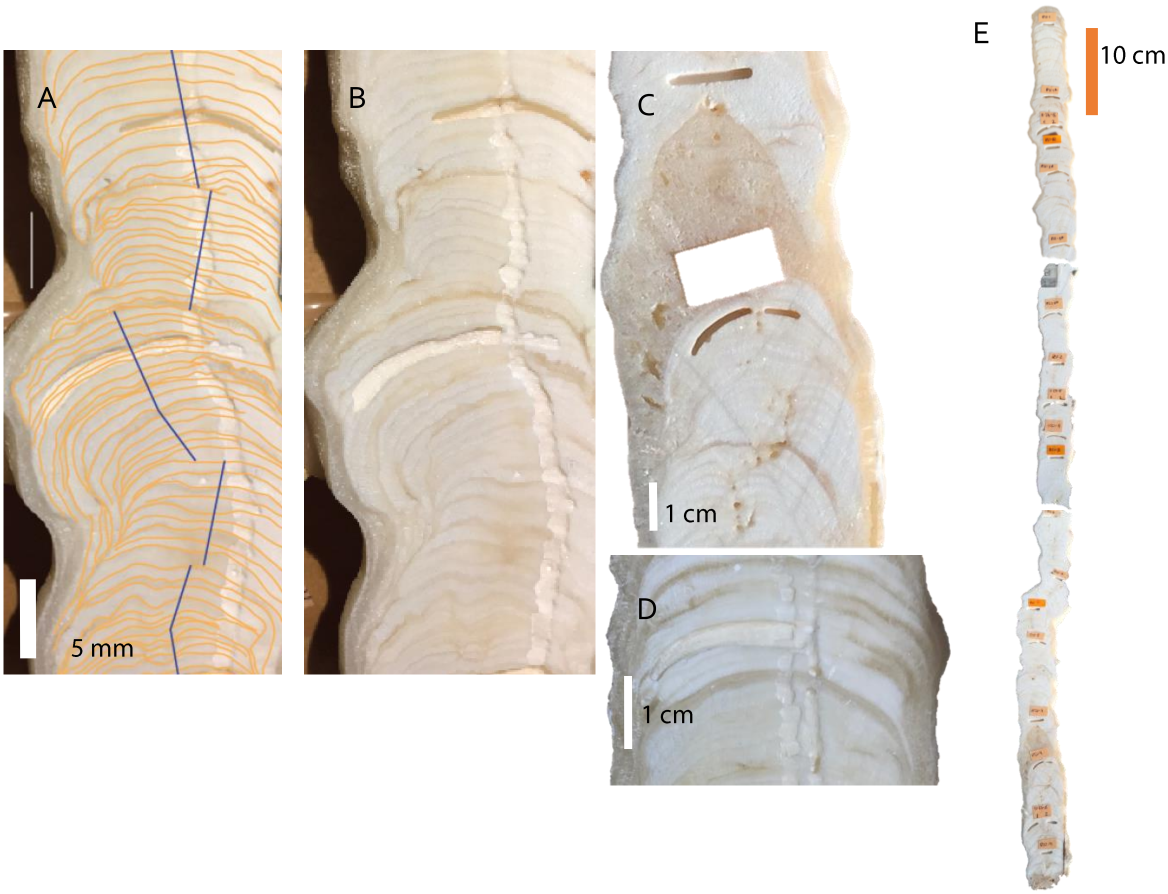


*Figure 3. Images of Yáax, a meter-long, mid-Holocene stalagmite from the YP A. Detail of mm-scale layers. Individual layers (orange) are deposited from bottom to top, with visible changes in thickness over time and changes in hypothesized growth axes (straight lines). B. Same as A, without annotations. C. Relatively dark and porous region without visible layers (surrounding the white rectangle); D. Hypothesized hiatus near the top of Yáax. E. Full stalagmite.*

### *2.3 Stable isotope measurements ($\delta^{18}O$ and $\delta^{13}C$)*

Calcite samples for stable isotope analysis were drilled at a ~2 mm resolution in a continuous track parallel to the growth axis (n = 342 samples). The $\delta^{18}O$ and $\delta^{13}C$ analyses were carried out using a Thermo Scientific MAT253 Stable Isotope Ratio Mass Spectrometer online coupled to a Kiel IV at University of California Santa Barbara. About 40-50 μg of each sample were reacted using 105% phosphoric acid addition. The evolving $CO_2$ was cryogenically cleaned before introduction into the mass spectrometer. The $\delta^{18}O$ and $\delta^{13}C$ data are reported on the Pee Dee

Belemnite (PDB) scale. The precision of the $\delta^{18}O$ and $\delta^{13}C$ analysis, assessed by analyzing NBS 19 standards, is ±0.07‰ and ±0.05‰ (2SE), respectively.

*2.4 Mg/Ca and Sr/Ca measurements*

Additional samples (weight = ~2 mg) were drilled for trace element analysis at a ~2 mm resolution in similar locations as the stable isotope powders (Section 2.3). Each sample was dissolved and diluted with 3% nitric acid. Standards with similar Mg/Ca and Sr/Ca ratios and concentrations were prepared using single-element standards. Analyses of Mg, Sr, and Ca were performed at MIT on an Agilent 7900 ICP-MS in no-gas mode. Data were corrected for blank intensities, isotopic abundances, and instrumental drift. Relative deviation in standards during one day of analysis averaged 4% (n = 5 standards per day) after these corrections. Replicate runs of identical solutions on different days also varied by an average of 4%. Replicate powders drilled from the same depth, but at different distances from the growth axis, varied by 1% or less in both Mg/Ca and Sr/Ca. All future references to trace elemental ratios in this work will be referring to Mg/Ca and Sr/Ca.

*2.5 Data analysis*

We used principal component (PC) analysis (based on all four geochemical proxy records, normalized and resampled to annual resolution) to find 4 PCs that explain 99% of the variance in the geochemical data (88% of the variance within PC1-3). We then analyzed the periodicity of the PCs using the periodogram function in MATLAB (version R2018b). We determined the statistical significance of periods using a null model with no true periodicity; we repeatedly (n = 2000 iterations) generated sets of four annual "records" with red noise (each record matching the variance of one proxy), then extracted the first PC from each set and normalized it. This is similar to checking the significance with an AR1 noise signal (Feng et al., 2014; Pollock et al., 2016), but with more iterations. The 2000 noise-based PCs were analyzed for periodicity, including 80%, 90%, and 95% confidence intervals (CI), and compared to the real PCs. Any peaks in spectral power above the 90% CI line are considered significant.

We also used Spearman's rank correlation, a non-parametric correlation analysis, to test for relationships between the proxies. We used a two-tailed correlation and p-values < 0.05 were considered significant.

**Results**

*3.1 U-Th dating and age model development*

*3.1.1 Initial dating analysis*

This stalagmite has precise age control, with age model uncertainty substantially lower than those found in nearby stalagmites of similar age due to its low detrital Th content (*e.g.* Akers et al., 2016; Pollock et al., 2016; Table 1). Therefore, Yáax and Itzamna are the oldest stalagmite records from the YP with dating errors <100 years (Medina-Elizalde et al., 2017).

*3.2 Stable isotopes*

*3.2.1 Comparison to modern drip water*

We sampled Yáax continuously at 2 mm resolution (n = 342 samples) in a region of the speleothem modeled to span 455 years, meaning that each sample averaged ~1.3 years; all proxy data were resampled to annual resolution to remove potential effects of sampling frequency and variable growth rate. Mean $\delta^{18}O_{calcite}$ was -5.5 ± 0.047‰ and mean $\delta^{13}C_{calcite}$ was -9.2 ± 0.091‰ (n = 455 points; mean ± 2SE). All subsequent data are reported at resampled resolution.

The average modern $\delta^{18}O_{drip}$ in the RS cave system is -3.9 ± 0.2‰ (VSMOW; ± 2SE). Using the Tremaine et al. (2011) equation for equilibrium fractionation and a temperature of 24.5˚C, we calculate that equilibrium precipitation of calcite would yield $\delta^{18}O_{calcite}$ = -4.8‰. This value overlaps with $\delta^{18}O_{calcite}$ in the late Holocene stalagmite (Itzamna $\delta^{18}O_{calcite}$ = -4.8 ± 0.1‰; mean ± 2SE) within error, suggesting ~equilibrium precipitation.

For a back of the envelope calculation of potential drip water composition in the mid-Holocene, we assume that no change in calcification temperature (*i.e.* mean cave air temperature was still ~24.5˚C). The reversed Tremaine et al. (2011) equilibrium calculation, using $\delta^{18}O_{calcite}$ = -5.5‰, suggests $\delta^{18}O_{drip}$ would have been approximately -4.6‰. This more negative value (in comparison to modern drip water, -3.9‰) supports the hypothesis that the mid-Holocene was wetter.

*3.2.2 Timeseries analysis*

$\delta^{18}O_{calcite}$ and $\delta^{13}C_{calcite}$ are significantly correlated with each other in Yáax (Figures 4 and 5; $\rho$ = 0.507, $p << 0.001$). Although some research has linked covariation in $\delta^{18}O$ and $\delta^{13}C$ to kinetic fractionation (*e.g.* Lachniet et al., 2004), previous work in this cave found that kinetic fractionation was not significant and that relative humidity is near 100% throughout the year (Lases-Hernandez et al., 2019; Medina-Elizalde et al., 2016a); therefore, we assume that both $\delta^{18}O_{calcite}$ and $\delta^{13}C_{calcite}$ primarily reflect hydrologic variability.

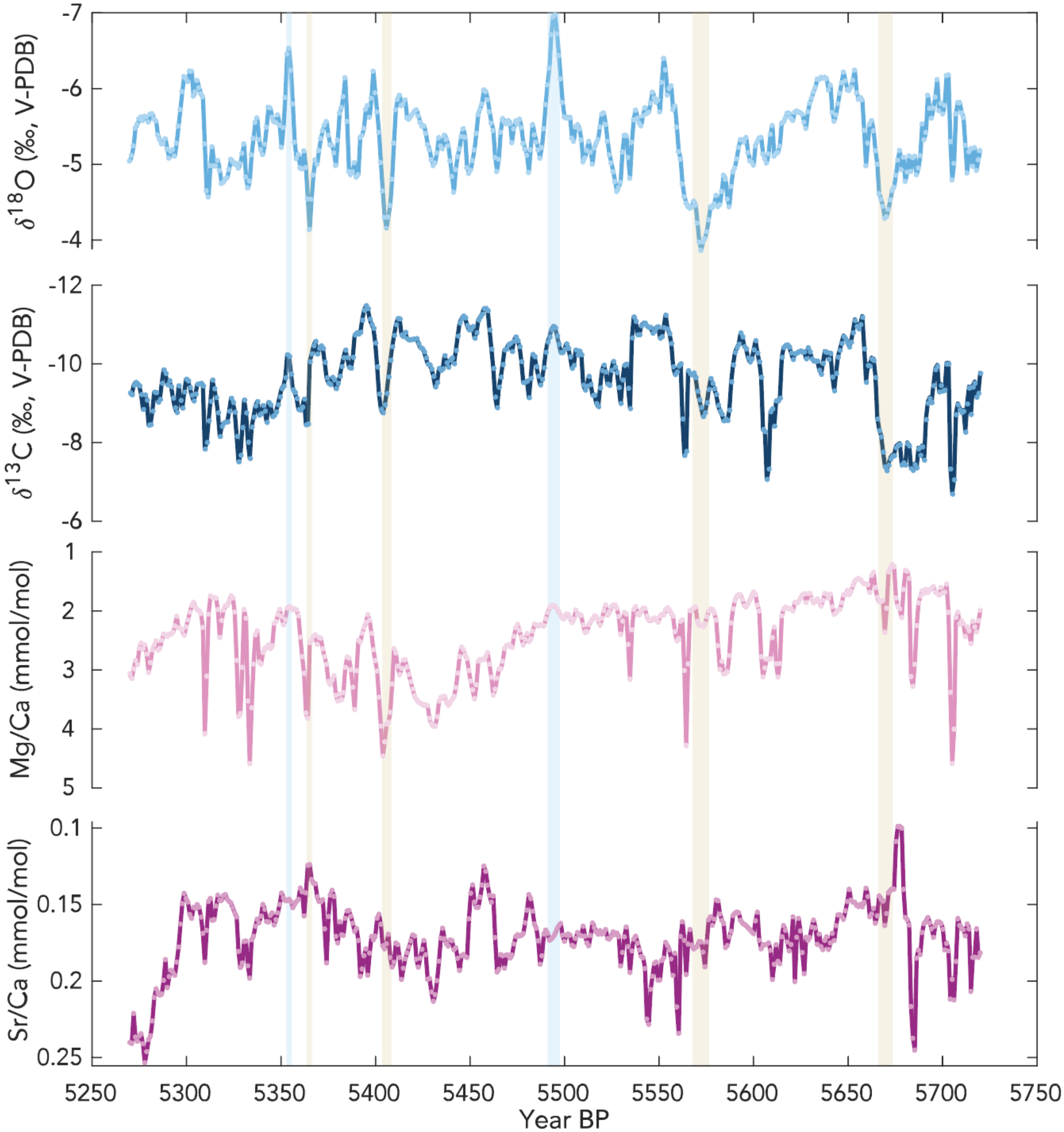


*Figure 4. Proxies analyzed in the studied stalagmite. $\delta^{18}O$, $\delta^{13}C$, Mg/Ca and Sr/Ca data for the growth period of Yáax, a stalagmite from the Yucatán Peninsula, resampled to annual resolution. Vertical bars highlight periods with $\delta^{18}O$ values at least 2 standard deviations greater than (tan) or less than (blue) the mean.*

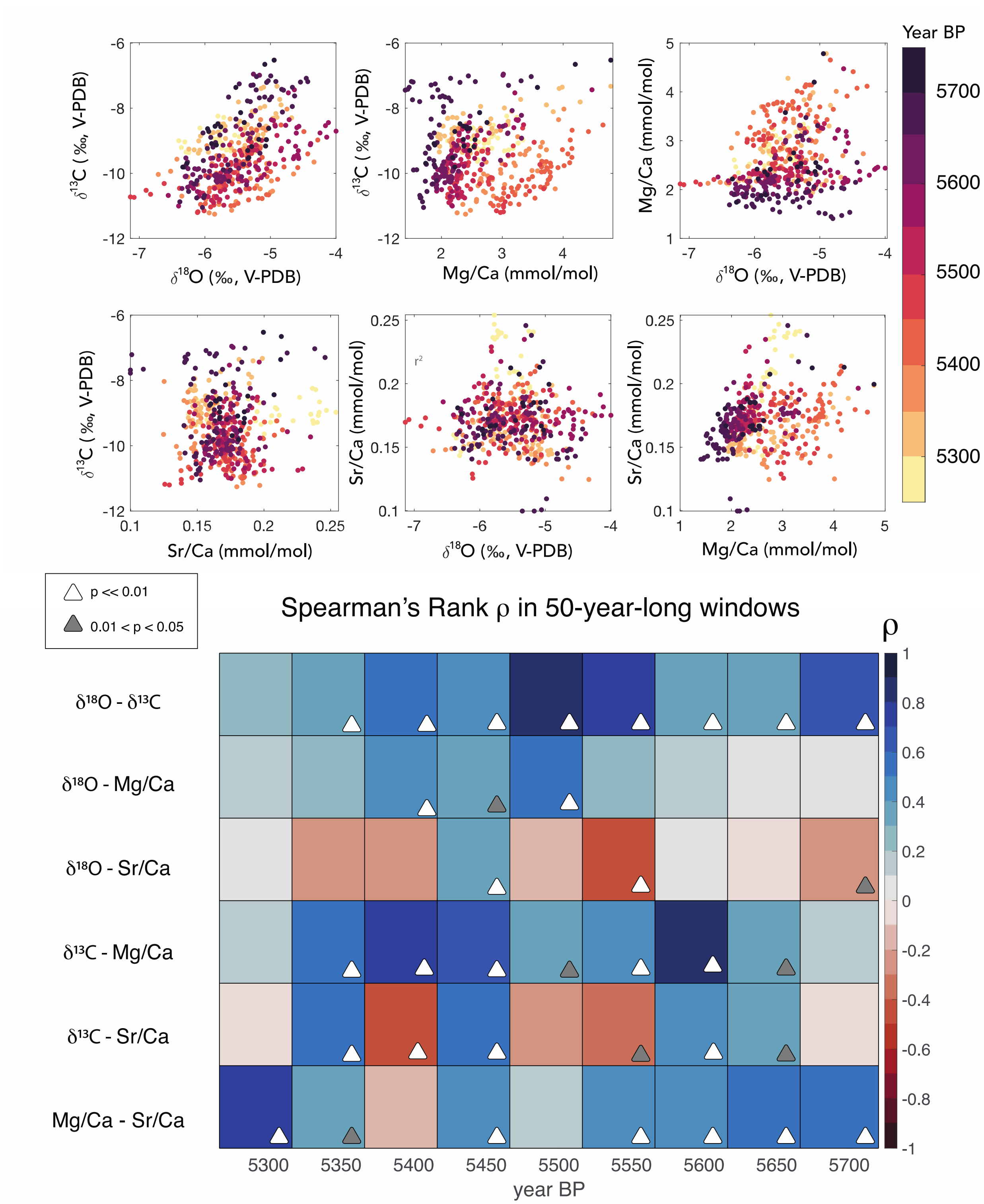


*Figure 5. Top: Cross plots showing linear regressions of trace element to calcium ratios and stable isotope data measured in Yáax. All data have been resampled to annual resolution to remove sampling bias and are colored according to their age. Bottom: Correlation coefficient (ρ) for Spearman's rank correlation tests on 50-year-long windows.*

*3.3 Trace elements*

*3.3.1 Results*

Our results show that mean mid-Holocene Mg/Ca was 2.6 ± 0.060 mmol/mol and Sr/Ca was 0.17 ± 0.0021 mmol/mol (±2SE). Broadly speaking, the two records have a similar shape, but behave somewhat differently at high resolution, yielding a low statistical correlation. More quantitatively, Spearman's rank correlations showed a weak but significant correlation between Mg/Ca and Sr/Ca data ($\rho = 0.34$, p-value << 0.01; Figure 5), meaning that Mg and Sr share some common controls. The youngest 50 years have the highest correlation ($\rho = 0.76$, p-value << 0.01), perhaps due to their synchronous increase toward higher values during that time period (Figure 4).

There is also low but significant correlation between Mg/Ca and $\delta^{18}O_{calcite}$ ($\rho = 0.25$, p-value << 0.01), but $\delta^{13}C$ and Mg/Ca had no significant correlation in the overall record ($\rho = 0.08$, p-value = 0.07)(Figure 5). Regressions between Sr/Ca and stable isotope data were not significant, yielding $|\rho| < 0.06$ and p-values > 0.2 (Figure 5).

It may be more informative to look at correlations within shorter windows, rather than in the full record, to allow for changes in the initial trace element composition of dripwater through time. For example, around 5400 yr BP, there is a synchronous visible spike in $\delta^{18}O$, $\delta^{13}C$, and Mg/Ca, but not in Sr/Ca (Figure 4, noted with tan bar). Between 5415 and 5366 yr BP, there are significant positive correlations between all three proxies with obvious increases, and not with Sr/Ca (Figure 5b). In fact, there is a significant negative correlation between $\delta^{13}C$ and Sr/Ca (Figure 5b). The increased ratios during this spike suggest that a multi-decade-long period with drier hydroclimate occurred, which we report with high confidence because of the significant correlations between the proxies. Similar periods of elevated Mg/Ca, $\delta^{13}C$ and $\delta^{18}O$ occur multiple times throughout the record, including around 5310-5340, 5360, 5570, and 5670 yrs BP. This association between peaks in Mg/Ca and $\delta^{13}C$ ratios and periods of high $\delta^{18}O$ supports the interpretation of $\delta^{18}O$ as reflecting local moisture availability.

There are several other instances where Mg/Ca and Sr/Ca increase dramatically, sometimes as much as two-fold. In general, many of the peaks or spikes in trace element ratio values coincide with elevated (drier) stable isotope values, though the Sr/Ca response appears to be weaker (Figures 4 and 5). Statistically, Sr/Ca and Mg/Ca are more similar to $\delta^{13}C$ than to $\delta^{18}O$: trace element ratios and $\delta^{13}C$ are significantly positively correlated in more 50-year-long windows (Sr/Ca = 4/9, Mg/Ca = 7/9) than trace elements and $\delta^{18}O$ (Sr/Ca = 1/9, Mg/Ca = 3/9)(Figure 5).

One example of differing $\delta^{18}O$ behavior occurs around 5550 yr BP, where $\delta^{13}C$, Sr/Ca, and Mg/Ca all spike a few years after the most significant increase in $\delta^{18}O$ (Figure 4, noted with tan bar). These anomalies could be related to threshold behavior in the epikarst, meaning that prior calcite precipitation, water-rock interactions, and degassing, and therefore increases in Sr/Ca, Mg/Ca, and $\delta^{13}C$, happen more slowly than the $\delta^{18}O_{precip}$ signal is transmitted to the stalagmite.

*3.3.2 Relationship with drip water trace element compositions*

Because this is the first record of Mg/Ca and Sr/Ca ratios in a stalagmite from the YP, it is important to compare modern drip water data to our paleo dataset to examine the potential relationship between them and determine the drivers of Mg/Ca and Sr/Ca in the stalagmite sample.

We used the Day and Henderson (2013) equations for $D_{Mg}$ and $D_{Sr}$ to calculate expected calcite trace element ratios given modern drip water [Mg] and [Sr]. Seepage drips had a minimum Mg/Ca of 58 mmol/mol and minimum Sr/Ca of 0.33 mmol/mol (n = 2 drip sites) (Lases-Hernandez, in prep.). Seasonal drips had a minimum Mg/Ca of 56 mmol/mol and minimum Sr/Ca of 0.58 mmol/mol (n = 1 drip site)(Lases-Hernandez, in prep.). We then performed a Rayleigh calculation using these drip water trace element ratios as starting concentrations. Modeled Mg/Ca and Sr/Ca values for seepage- and seasonal-type drips overlapped with measured calcite data (Supplementary Information).

The calcite data overlap with modeled ratios for ~30-60% prior calcite precipitation. Regression of the calcite Mg/Ca and Sr/Ca data in log space yielded a nearly flat slope (m = 0.17; Figure 6B). This result suggests that PCP was not the dominant control on Mg/Ca and Sr/Ca during the mid-Holocene (Sinclair et al., 2012). Instead, the regression yields a slope similar to that reported to relate to water-rock interactions (m = 0.18), including calcite recrystallization (Sinclair et al., 2012). Therefore, calcite recrystallization could be the main driver of variability in Mg/Ca and Sr/Ca ratios (Sinclair et al., 2012).

When considered alongside the stable isotope data that suggest a wetter hydroclimate during the mid-Holocene, the lack of evidence for PCP in trace element ratios from Yáax supports the hypothesis of increased precipitation in comparison to the late Holocene and the modern. Therefore, trace element to calcium ratios provide an independent tool to assess whether the stable isotope data primarily reflect hydrological changes in RS.

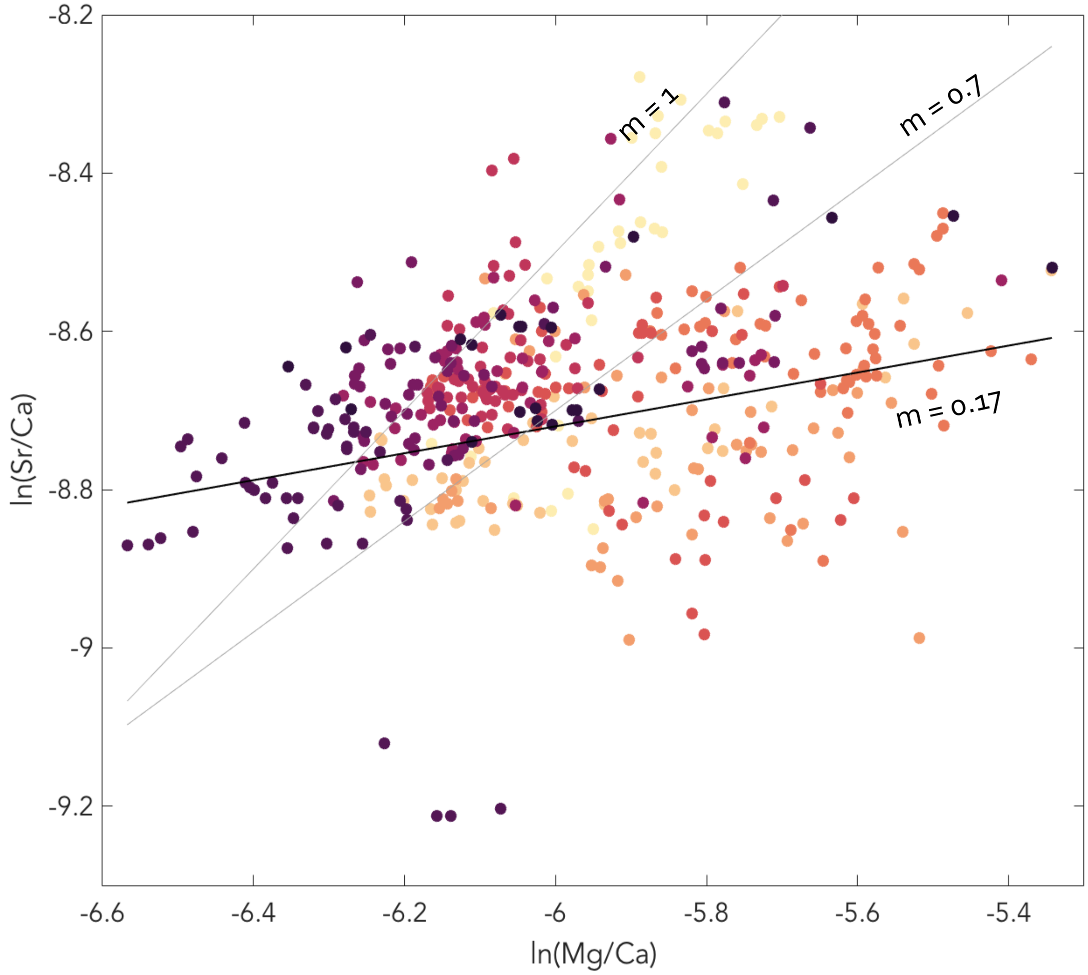


*Figure 6. Linear regression of Sr/Ca and Mg/Ca ratios for Yáax. The Yáax data have a nearly flat slope (m = 0.17). Higher slopes (m = 0.7 – 1) associated with prior calcite precipitation (Sinclair et al., 2012) are shown for reference, but do not match the Yáax data.*

### *3.4. Spectral Analysis*

In order to compare mid-Holocene precipitation variability to late Holocene variability, we used spectral analysis to determine periodicity in the four principal components (PCs) from Yáax geochemical proxy data. We assume that all the PCs reflect hydroclimate variability. All four PCs were significantly correlated with the original geochemical records (p-value << 0.001; Supplementary Information).

Spectral analysis revealed periods of ~20 years$^{-1}$, ~10 years$^{-1}$, and ~5 years$^{-1}$ present at the 90% CI in multiple PCs (Figure 7). At the 80% CI, an additional period of 50 years$^{-1}$ was noted (Figure 7).

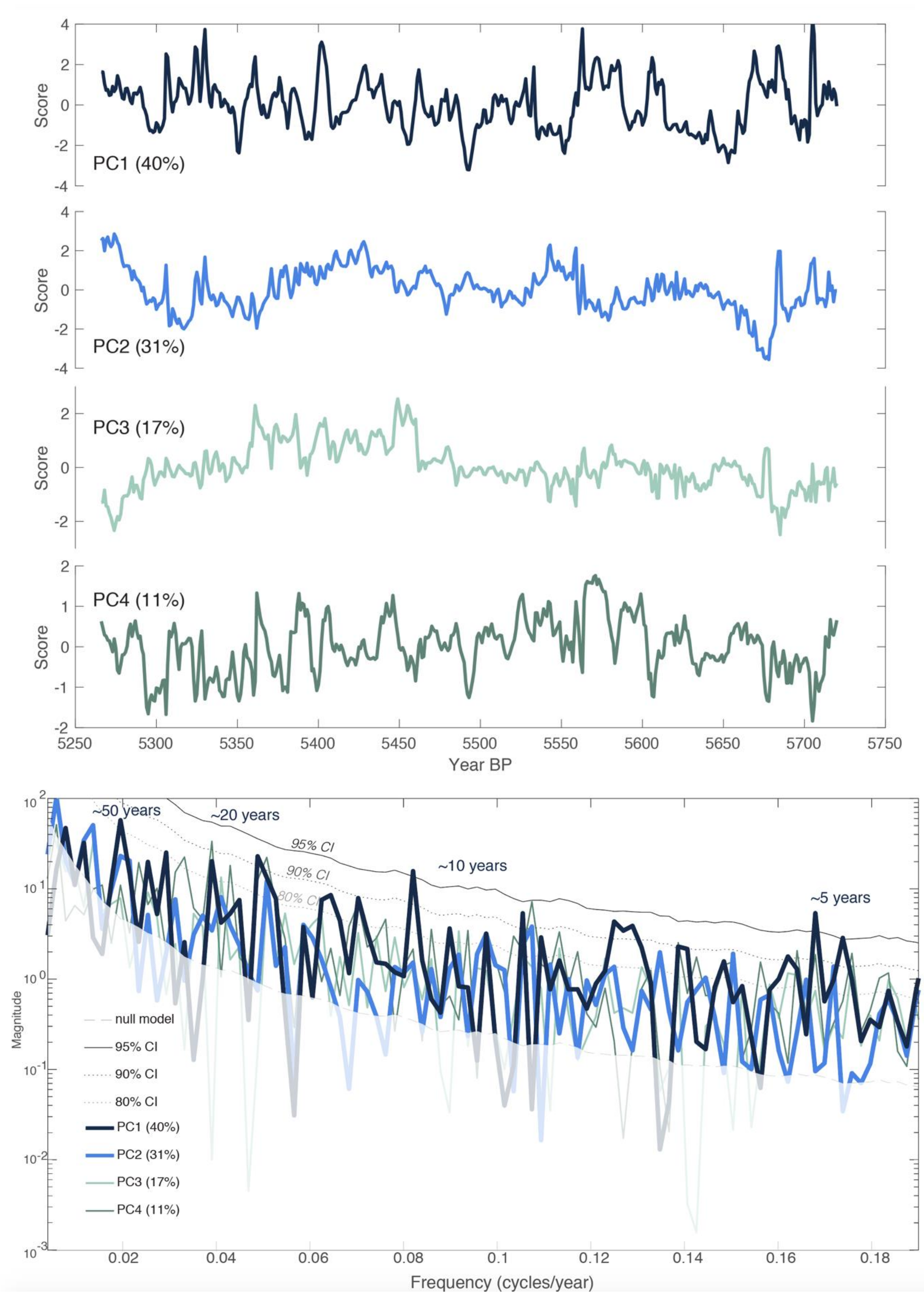


*Figure 7. Top. Principal components (PCs) of normalized geochemical data (oxygen isotope, carbon isotope, Mg/Ca, and Sr/Ca ratios) from Yáax. Legend shows variance explained by each PC. Bottom. Spectral analysis of PCs shown in the top panel, with black lines denoting confidence intervals from a red noise-based null model. There are cycles with periods of ~20, 10, and 5 years present at the 90% CI.*

*3.5 Comparison to other records*

Although there are several existing paleoclimate records from the YP region (see Section 1 for a summary), in-depth analysis in this study is restricted to Itzamna, a stalagmite from RS that grew during a more recent time period than Yáax (~3000 – 1500 years BP). Because these two stalagmites came from the same cave and have similar dating errors, comparing them allows for a more robust analysis of precipitation variability and amount over time. The Itzamna $\delta^{18}O$ record has a lower resolution, so the higher resolution Yáax $\delta^{18}O$ record was smoothed for comparison (5-point moving average).

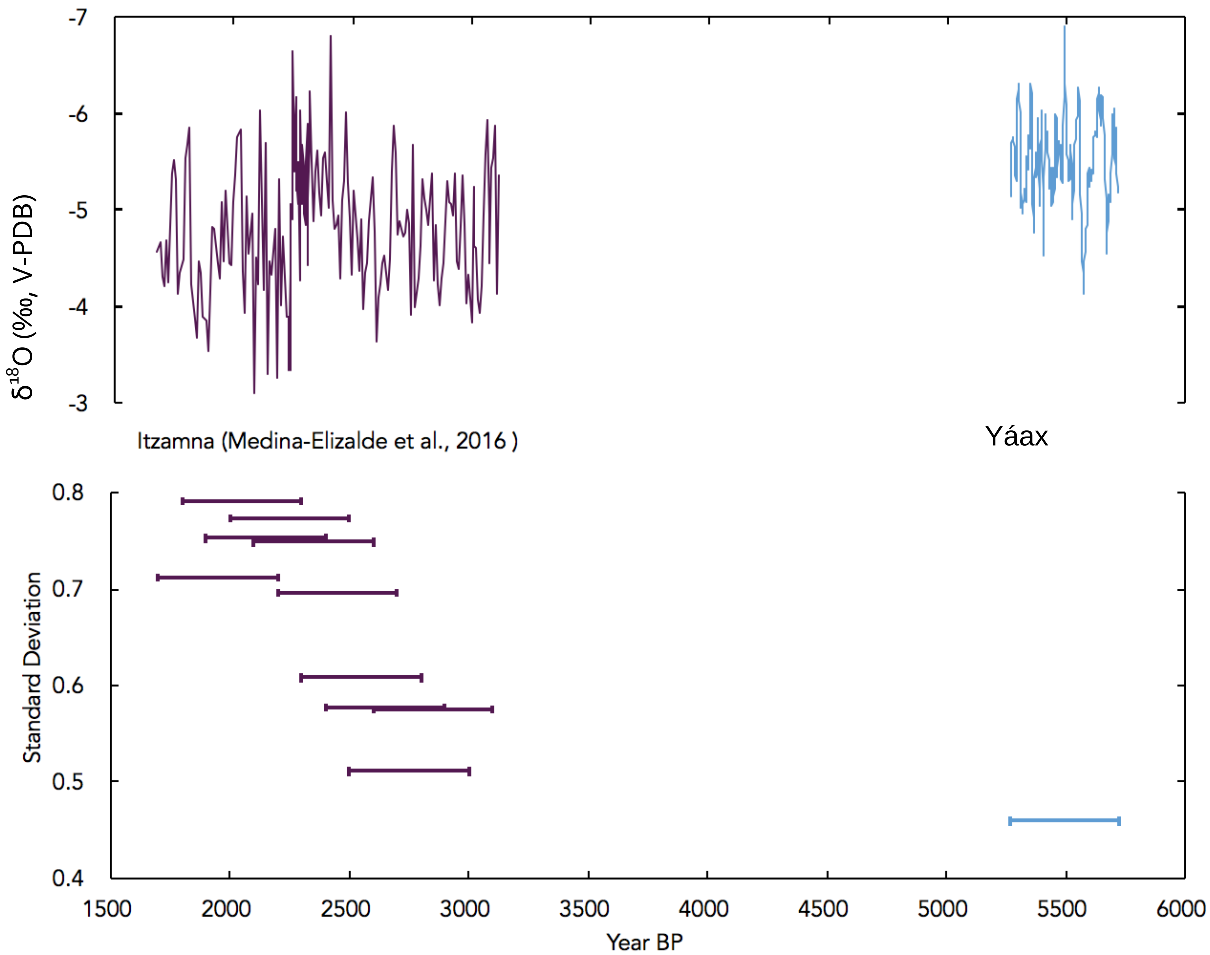


*Figure 8. Time series records of $\delta^{18}O_{calcite}$ in Itzamna (Medina-Elizalde et al., 2016a) and Yaax. B. Standard deviation of 500-year-long snapshots of $\delta^{18}O_{calcite}$ from Itzamna (Medina-Elizalde et al., 2016a) and Yáax (5-point smoothed to more closely match sampling resolution of Itzamna), two stalagmites from the same cave. Variability is significantly lower in Yaax than in Itzamna (F-test, $p << 0.001$) and median $\delta^{18}O$ is significantly different (Mann-Whitney U-test, $p << 0.001$).*

The median $\delta^{18}O_{calcite}$ for Itzamna was -4.9‰, significantly less negative than Yaax's median $\delta^{18}O_{calcite}$ = -5.5‰ (Figure 8; Mann-Whitney U-test, $p << 0.001$). The variance in the two stalagmites is also statistically different (F-test, $p << 0.001$), with Yáax showing less variability than Itzamna (Figure 8). The variability in Itzamna increased over time, but was always greater than that of Yáax (Figure 8). As expected, Yáax's variance was slightly higher without smoothing (variance = 0.25 unsmoothed or 0.21 smoothed), but was still significantly lower than that of Itzamna (F-test, $p << 0.001$)

## Discussion

*4.1 Mid-Holocene hydrological variability in the Yáax record*

Based on evidence from previous studies conducted in RS and the observed correlation between oxygen and carbon stable isotope ratios and trace elements, we suggest that $\delta^{18}O_{calcite}$ reflects precipitation amount in this region.

There are notable dry periods (more positive ratios, greater than 2SD above mean $\delta^{18}O_{calcite}$) around 5675 and 5575 yr BP, which appear to have lasted for 20-50+ years, and two shorter dry intervals around 5400 and 5300 yr BP. The duration of observed dry periods is consistent with spectral analysis showing 20-40 year periods in all PCs, as well as longer cycles (50+ years). We note that some Mesoamerican droughts in both the Common Era and the past century had similar multi-decadal lengths (*e.g.* Medina-Elizalde et al., 2016a). This similarity shows that multi-decadal precipitation cycles are an integral feature of YP hydroclimate, occurring even during a period of inferred higher mean precipitation and reduced precipitation variance.

Both of the long dry periods have a sawtooth pattern in the $\delta^{18}O_{calcite}$, with slow drying and a rapid change back to wetter conditions. Although the $\delta^{18}O_{calcite}$ was only outside the $2\sigma$ envelope briefly (a few years at the hypothesized maximum of the dry period), the slow drying lasted for decades. The trace element to calcium ratios and $\delta^{13}C_{calcite}$ don't follow the same sawtooth shape; instead, they have a few sharp increases during the hypothesized dry periods.

Taken together, the qualitative agreement and the statistical correlations between trace elements and stable isotopes show that it is feasible to use Mg/Ca and Sr/Ca as paleoclimate proxies in this region. Furthermore, we suggest that it is prudent to collect data on all four proxies because they record hydrological variability in different ways, potentially enriching the interpretation of the record.

*4.2 Comparison to other records*

Analysis of Yáax compared to Itzamna showed decreased variability and increased mean $\delta^{18}O$ in the mid-Holocene (compared to the late Holocene). Because both samples come from the same cave, we assume that the differences in the variability of both $\delta^{18}O$ records are only due to changes in hydroclimate over time and not due to temperature variance or inter-cave differences, as might be the case when using stalagmites from two different caves for temporal comparisons.

Therefore, we conclude that the YP was experiencing significantly different climate patterns between the late Holocene and the mid-Holocene. Lower average $\delta^{18}O_{calcite}$ during the mid-Holocene (Yáax growth period) suggests that there was more precipitation than during the late Holocene. Trace element ratios with a lack of evidence for PCP also support the hypothesized wetter mid-Holocene, as the aquifer may have been too wet for PCP to occur in the epikarst.

These observations are consistent with results from previous stalagmite studies in Belize that found wetter, less variable mid-Holocene hydroclimate (*e.g.* Metcalfe et al., 2009; Pollock et al., 2016) in comparison to the later Holocene. Lacustrine records from the YP also showed higher mid-Holocene lake levels (Hodell et al., 1995; Whitmore et al., 1996), and a series of calcite rafts from other caves in the YP show progressive drying from 7,000 years BP to the present (Kovacs et al., 2017). Regional agreement among these paleoclimate records, across proxies and archives, suggests that the driver of increased precipitation amount and decreased precipitation variability is not isolated to this cave site or restricted to this short interval of the mid-Holocene. Instead, the driver(s) is at least regional in scale, and persisted for several thousand years.

Increased precipitation amount is likely due (in part) to increased seasonality during the mid-Holocene, which preferentially warmed North Atlantic summer SSTs, promoting increased YP precipitation via enhanced moisture transport by the CLLJ and a more northerly mean position of the ITCZ. This pattern has been observed in the instrumental record and model simulations (Bhattacharya et al., 2017), and has been invoked to explain other observed proxy records (Ridley et al., 2015; Pollock et al., 2016).

Increased tropical cyclone activity could also have played a part in increasing YP precipitation in the mid-Holocene. Pausata et al. (2017) modeled tropical cyclone activity at 6 kyr BP and demonstrated that increased seasonality, a vegetated Sahara, and a reduction in Saharan dust emissions could lead to an increase in tropical cyclones during the mid-Holocene, especially in the Caribbean. Though we cannot resolve individual high-precipitation events in our record, our results are consistent with increased frequency of tropical cyclones from 5.7 to 5.2 kyr BP, compared to the late Holocene and pre-industrial periods.

Lower precipitation variability during the mid-Holocene could be related to reduced ENSO variability. Several studies have shown that the mid-Holocene was a period of reduced ENSO variance compared to the late Holocene (Carré et al., 2014; Chen et al., 2016; Emile-Geay et al., 2016; Koutavas et al., 2006; Koutavas and Joanides, 2012). Summer CLLJ variability is thought to be linked to tropical Pacific variability (Muñoz et al., 2008), so decreased Pacific SST variability could lead to a more stable CLLJ, yielding the diminished precipitation variation we observe in Yáax.

Previous modeling, monitoring, and proxy data have suggested that ENSO mean state influences tropical Atlantic cyclone formation (Elsner et al., 1999; Frappier et al., 2014; Lases-Hernandez et al., 2019; Medina-Elizalde et al., 2016b; Wu & Lau, 1992). Therefore, decreased ENSO variability during the mid-Holocene could reduce changes in the frequency of tropical cyclones, further decreasing the amplitude of precipitation variability in the YP.

Our study contributes to a wide range of work linking Atlantic Multidecadal Variability (AMV) to Caribbean and Gulf of Mexico hydroclimate (Alexander et al., 2014; Battacharya et al., 2017; Karmalkar et al., 2011; Knight et al., 2006). Instrumental, paleoclimate, and modeling data also support a link between Atlantic Multidecadal Variability (AMV) and hydroclimate over multiple other regions, including the North Atlantic (Knight et al., 2006), northeastern Brazil (Sutton et al., 2005), African Sahel (Folland et al., 1986; Rowell et al., 1992), western Europe (Folland et al., 1986; Knight et al., 2006; Sutton et al., 2005), and North America (Fensterer et al., 2012;

Folland et al., 2001; Medina-Elizalde et al., 2017). Future work should examine whether paleoclimate records with decadal-scale resolution from these other regions also show reduced variance in the mid-Holocene relative to the late Holocene.

Regardless of the climate dynamics at play, the 20 – 50 yr cyclicity and rapid drying observed in Yáax indicate significant multidecadal wet-dry cycles, much like there are in the present and late Holocene YP, despite the wetter, warmer climate state. Thus, we expect similar, multidecadal droughts both under future climate warming and in other paleoclimate records from this region, including others that overlap with shifts in ancient Maya society.

## 5 Conclusions

### *5.1 Summary*

In this study, we have presented a precisely-dated, high-resolution multi-proxy YP paleoclimate record spanning a 455-year-long interval (5720 - 5266 yr BP) of the mid-Holocene. The record is consistent with previous observations of increased precipitation in the mid-Holocene compared to the late Holocene. Results from this study suggest that multi-decadal precipitation variations were a persistent feature in regional hydroclimate during the mid-Holocene, just as they were in the past 2 millennia, but with reduced amplitude. Because the mid-Holocene had a different climate mean state (more summer solar input and higher mean precipitation) than the late Holocene, we conclude that background climate can impact precipitation variability in the YP. We suggest that mid-Holocene reductions in ENSO and/or AMV variability, driven by altered seasonality, led to more stable YP precipitation patterns. As background climate changes under anthropogenic warming conditions, it will be important to model predicted changes in precipitation mean and variance. Models of future hydroclimate can be tested by comparing predicted variance at 6 kyr BP to that recorded in other proxy records and 6 kyr models.

Although stalagmites provide only a short snapshot of hydroclimate during their growth period, this study demonstrates the utility of single-cave, multi-stalagmite analyses, especially when considering changes in variability over time. This work presents the first record of stalagmite Mg/Ca and Sr/Ca ratios in the Yucatán Peninsula. Our results support the inclusion of trace element ratios in stalagmites that cover changes in ancient Maya civilization to provide additional climate information. These results are a step forward in YP paleoproxy interpretations and provide a better understanding of controls on precipitation amount and variability.

## 6 Acknowledgements

Data generated in this study are available in the NOAA/WDS archive (https://www.ncdc.noaa.gov/paleo/study/29211) and supplemental information *[NOTE: URL set to private until acceptance]*. Data from Itzamna are available as supplementary data in Medina-Elizalde et al. (2016a), and drip water data from Lases-Hernandez (in prep.) will be available in May upon thesis submission.

This work was funded by US National Science Foundation grants AGS-1702848 (M. Medina-Elizalde) and AGS–1502877 (S. Burns). This material is based upon work supported by the National Science Foundation Graduate Research Fellowship (G. Serrato Marks). Additional support was provided by the MIT EAPS Student Research Fund and the WHOI Ocean Ventures Fund. We appreciate Nick Scroxton's work on XRD analysis and statistical insights, and Sarah

Weidman's contribution to drilling at MIT. Finally, we thank the staff at Río Secreto Cave for their assistance.

**References**

Akers, P. D., Brook, G. A., Railsback, L.B., Liang, F., Iannon, G., Webster, J.W., et al. (2016). An extended and higher-resolution record of climate and land use from stalagmite MC01 from Macal Chasm, Belize, revealing connections between major dry events, overall climate variability, and Maya sociopolitical changes. *Palaeogeography, Palaeoclimatology, Palaeoecology*, **459**, 268-288. https://doi.org/10.1016/j.palaeo.2016.07.007

Bhattacharya, T., Chiang, J., & Cheng, W. (2017) Ocean-atmosphere dynamics linked to 800–1050 CE drying in Mesoamerica. *Quaternary Science Reviews* **169**, 263–277. https://doi.org/10.1016/j.quascirev.2017.06.005

Breitenbach, S. F. M, Rehfeld, K., Goswami, B., Baldini, J. U. L., Ridley, H.E., Kennett, D. J., et al. (2012). Constructing proxy records from age models (COPRA). *Climate of the Past* **8,** 1765-1779. https://doi.org/10.5194/cp-8-1765-2012

Burns, S. J., Matter, A., Frank, N., & Mangini, A. (1998). Speleothem-based paleoclimate record from northern Oman. *Geology*, **26**(6), 499-502. https://doi.org/10.1130/0091-7613(1998)026%3C0499:SBPRFN%3E2.3.CO;2

Burns, S. J., Godfrey, L. R., Faina, P., McGee, D., Hardt, B., Ranivoharimanana, L., & Randrianasy, J. (2016). Rapid human-induced landscape transformation in Madagascar at the end of the first millennium of the Common Era. *Quaternary Science Reviews*, **134**, 92–99. https://doi.org/10.1016/j.quascirev.2016.01.007

Bush, M. B., Correa-Metrio, A. Y., Hodell, D. A., Brenner, M., Anselmetti, F. S., Ariztegui, D., et al. (2009). Re-evaluation of Climate Change in Lowland Central America During the Last Glacial Maximum Using New Sediment Cores from Lake Petén Itzá, Guatemala (pp. 113–128). https://doi.org/10.1007/978-90-481-2672-9_5

Carré, M., Sachs, J. P., Purca, S., Schauer, A. J., Braconnot, P., Falcón, R. A., et al. (2014). Holocene history of ENSO variance and asymmetry in the eastern tropical Pacific. *Science*, **345**(6200), 1045-1048. https://doi.org/10.1126/science.1252220

Chen, S., Hoffmann, S. S., Lund, D. C., Cobb, K. M., Emile-Geay, J., & Adkins, J. F. (2016). A high-resolution speleothem record of western equatorial Pacific rainfall: Implications for Holocene ENSO evolution. *Earth and Planetary Science Letters*,**442,** 61-71. https://doi.org/10.1016/j.epsl.2016.02.050

Cruz, F. Burns, S. J., Jercinovic, M., Karmann, I., Sharp, W. D., & Vuille, M. (2017) Evidence of rainfall variations in Southern Brazil from trace element ratios (Mg/Ca and Sr/Ca) in a Late Pleistocene stalagmite. *Geochimica et Cosmochimica Acta* **71**, 2250–2263. https://doi.org/10.1016/j.gca.2007.02.005

Dansgaard, W. (1964) Stable isotopes in precipitation. *Tellus*, **16**, 436–468. https://doi.org/10.1111/j.2153-3490.1964.tb00181.x

Day, C. C, & Henderson, G. M. (2013) Controls on trace-element partitioning in cave-analogue calcite. *Geochimica et Cosmochimica Acta*, **120**, 612-627. https://doi.org/10.1016/j.gca.2013.05.044

Dee, S. G., Parsons, L. A., Loope, G. R., Overpeck, J. T., Ault, T. R., & Emile-Geay, J. (2017). Improved spectral comparisons of paleoclimate models and observations via proxy system modeling: Implications for multi-decadal variability. *Earth and Planetary Science Letters*, **476**, 34–46. https://doi.org/10.1016/j.epsl.2017.07.036

Douglas, P. M. J., Pagani, M., Canuto, M. A., Brenner, M., Hodell, D. A., Eglinton, T. I., & Curtis, J. H. (2015). Drought, agricultural adaptation, and sociopolitical collapse in the Maya Lowlands. *Proceedings of the National Academy of Sciences of the United States of America*. https://doi.org/10.1073/pnas.1419133112

Elsner, J. B., Kara, A. B., & Owens, M. A. (1999). Fluctuations in North Atlantic hurricane frequency. *Journal of Climate*, **12**(2), 427–437. https://doi.org/10.1175/1520-0442(1999)012<0427:FINAHF>2.0.CO;2

Emile-Geay, J., Cobb, K. M., Carré, M. Braconnot, P., Leloup, K., Zhou, Y., et al. (2016). Links between tropical Pacific seasonal, interannual and orbital variability during the Holocene. *Nature Geoscience*, **9**, 168-173. https://doi.org/10.1038/ngeo2608

Fairchild, I.J., Borsato, A., Tooth, A.F., Frisia, S., Hawkesworth, C. J., Huang, Y., et al. (2000). Controls on trace element (Sr-Mg) compositions of carbonate cave waters: implications for speleothem climatic records. *Chemical Geology*, **166(3-4)**, 255–269. https://doi.org/10.1016/S0009-2541(99)00216-8

Fairchild, I.J., Baker, A., Borsato, A., Frisia, S., Hinton, R.W., McDermott, F., & Tooth, A.F. (2001). Annual to sub-annual resolution of multiple trace-element trends in speleothems. *Journal of the Geological Society*, **158**(5), 831–841. https://doi.org/10.1144/jgs.158.5.831

Fensterer, C., Scholz, D., Hoffmann, D., Spötl, C., Pajón, J. M., & Mangini, A. (2012). Cuban stalagmite suggests relationship between Caribbean precipitation and the Atlantic Multidecadal Oscillation during the past 1.3 ka. *Holocene*, 22(12), 1405–1412. https://doi.org/10.1177/0959683612449759

Folland, C. K., Palmer, T. N., & Parker, D. E. (1986). Sahel rainfall and worldwide sea temperatures, 1901-85. *Nature*. https://doi.org/10.1038/320602a0

Folland, C. K., Colman, A. W., Rowell, D. P., & Davey, M. K. (2001). Predictability of northeast Brazil rainfall and real-time forecast skill, 1987-98. *Journal of Climate*. https://doi.org/10.1175/1520-0442(2001)014<1937:PONBRA>2.0.CO;2

Frappier, A. B., Sahagian, D., Carpenter, S. J., González, L. A., & Frappier, B. R. (2007). Stalagmite stable isotope record of recent tropic cyclone events. *Geology*, **35**(2), 111–114. https://doi.org/10.1130/G23145A.1

Frappier, A., Pyburn, J., Pinkey-Drobnis, A.D., Wang, X., Corbett, D.R., & Dahlin, B.H. (2014). Two millennia of tropical cyclone-induced mud layers in a northern Yucatán stalagmite: Multiple overlapping climatic hazards during the Maya Terminal Classic "megadroughts." *Geophysical Research Letters,* **41**(14), 5148–5157. https://doi.org/10.1002/2014GL059882

Genty, D., Baker, A., Massault, M., Proctor, C., Gilmour, M., Pons-Branchu, E., & Hamelin, B. (2001). Dead carbon in stalagmites: Carbonate bedrock paleodissolution vs. ageing of soil organic matter. Implications for 13C variations in speleothems, *Geochimica et Cosmochimica Acta*, **65**(20), 3443-3457. https://doi.org/10.1016/S0016-7037(01)00697-4

Genty, D., Blamart, D., Ghaleb, B., Plagnes, V., Causse, C., Bakalowicz, M., et al. (2006). Timing and dynamics of the last deglaciation from European and North African δ13C stalagmite profiles—comparison with Chinese and South Hemisphere stalagmites. *Quaternary Science Reviews*, **25**(17-18), 2118-2142. https://doi.org/10.1016/j.quascirev.2006.01.030.

Giannini, A., Kishnir, Y., & Cane, M. A. (2000). Interannual Variability of Caribbean Rainfall, ENSO, and the Atlantic Ocean. *Journal of Climate*, 32(18), 297-311. https://doi.org/10.1175/1520-0442(2000)013%3C0297:IVOCRE%3E2.0.CO;2

Hellstrom, J., McCulloch, M., & Stone, J. (1998). A detailed 31,000-year record of climate and vegetation change from the isotope geochemistry of two New Zealand speleothems. *Quaternary Research*, **50**, 167-178. https://doi.org/10.1006/qres.1998.1991.

Hodell, D. A., Curtis, J. H., & Brenner, M. (1995). Possible role of climate in the collapse of Classic Maya civilization. *Nature*, **375**(6530), 391–394. https://doi.org/10.1038/375391a0

Hodell, D. A., Brenner, M., & Curtis, J. H. (2005). Climate change on the Yucatan Peninsula during the little ice age. *Quaternary Research*, **63**, 109–121. https://doi.org/10.1016/j.yqres.2004.11.004.

Karmalkar, A. V., Bradley, R. S., & Diaz, H. F. (2011). Climate change in Central America and Mexico: regional climate model validation and climate change projections. Climate Dynamics, **37**, 605-629. https://doi.org/10.1007/s00382-011-1099-9

Knight, J. R., Folland, C. K., & Scaife, A. A. (2006). Climate impacts of the Atlantic multidecadal oscillation. *Geophysical Research Letters*, **33**(17). https://doi.org/10.1029/2006GL026242

Koutavas, A., deMenocal., P.B., Olive, G.C., & Lynch-Stieglitz, J. (2006). Mid-Holocene El Niño–Southern Oscillation (ENSO) attenuation revealed by individual foraminifera in eastern tropical Pacific sediments. *Geology*, **34**(12), 993-996. https://doi.org/10.1130/G22810A.1

Koutavas, A., Joanides, S. (2012). El Niño-Southern Oscillation extrema in the Holocene and Last Glacial Maximum. *Paleoceanography and Paleoclimatology*, **27**(4), PA4208. https://doi.org/10.1029/2012PA002378

Lachniet, M. S., Burns, S. J., Piperno, D. R., Asmerom, Y., Polyak, V., Moy, C. M., & Christenson, K. (2004). A 1500-year El Niño/Southern Oscillation and rainfall history for the isthmus of Panama from speleothem calcite. *Journal of Geophysical Research Atmospheres*, **109**(D20). https://doi.org/10.1029/2004JD004694

Lachniet, M. S., Asmerom, Y., Polyak, V., & Bernal, J. P. (2017). Two millennia of Mesoamerican monsoon variability driven by Pacific and Atlantic synergistic forcing. *Quaternary Science Reviews*, **155**, 100-113. https://doi.org/10.1016/j.quascirev.2016.11.012

Lases-Hernandez, F., Medina-Elizalde, M., Burns, S., & DeCesare, M. (2019). Long-term monitoring of drip water and groundwater stable isotopic variability in the Yucatán Peninsula: Implications for recharge and speleothem rainfall reconstruction. *Geochimica et Cosmochimica Acta*, **246**, 41-59. https://doi.org/10.1016/j.gca.2018.11.028

Lases-Hernandez, F, in prep. Characterization of geochemical and environmental processes that modulate the isotoic and elemental composition of drip water and calcite in Rio Secreto, a karstic system in the Yucatan Peninsula, Mexico (Spanish). Doctoral Thesis.

Laskar, J., Robutel, P., Gastineau, M., Correia, C. M., & Levrard, B. (2004). A long-term numerical solution for the insolation quantities of the Earth. *Astronomy and Astrophysics*, **428**(1), 261-285. https://doi.org/10.1051/0004-6361:20041335

Lechleitner, F. A., Breitenbach, S. F. M., Rehfeld, K., Ridley, H. E., Asmerom, Y., Prufer, K. M. et al. (2017). Tropical rainfall over the last two millennia: evidence for a low-latitude hydrologic seesaw. *Scientific Reports*, **7**(1), 45809. https://doi.org/10.1038/srep45809

Lewis, S. C., Gagan, M. K., Ayliffe, L. K., Zhao, J. X., Hantoro, W. S., Treble, P. C., & Suwargadi, B. W. (2011). High-resolution stalagmite reconstructions of Australian–Indonesian monsoon rainfall variability during Heinrich stadial 3 and Greenland interstadial 4. *Earth and Planetary Science Letters*, **303**(1-2), 133-142. https://doi.org/10.1016/j.epsl.2010.12.048

Marcott, S. A., Shakun, J. D., Clark, P. U., & Mix, A. C. (2013). A Reconstruction of Regional and Global Temperature for the Past 11,300 Years. *Science*, **339**(6124), 1198-1201. https://doi.org/10.1126/science.1228026

Marsicek, J., Shuman, B., Bartlein, P., Shafer, S. L., & Brewer, S. (2018). Reconciling divergent trends and millennial variations in Holocene temperatures. *Nature* **554**, 92–96. https://doi.org/10.1038/nature25464

McCabe, G. J., Palecki, M. A., & Betancourt, J. L. (2004). Pacific and Atlantic Ocean influences on multidecadal drought frequency in the United States. Proceedings of the National Academy of Sciences of the United States of America, 101(12), 4136–4141. https://doi.org/10.1073/pnas.0306738101

McGee, D., Donohoe, A., Marshall, J., & Ferreira, D. (2014). Changes in ITCZ location and cross-equatorial heat transport at the Last Glacial Maximum, Heinrich Stadial 1, and the mid-Holocene. *Earth and Planetary Science Letters*, 390, 69–79. https://doi.org/10.1016/j.epsl.2013.12.043

Medina-Elizalde, M., Burns, S., Lea, D., Asmerom, Y., von Gunten, L., & Polyak, V. (2010). High resolution stalagmite climate record from the Yucatán Peninsula spanning the Maya terminal classic period. *Earth and Planetary Science Letters*, **298**(1-2), 255-262. https://doi.org/10.1016/j.epsl.2010.08.016

Medina-Elizalde, M., Burns, S. J., Polanco-Martinez, J. M., Beach, T., Lases-Hernandez, F., & Shen, C. C. (2016a). High-resolution speleothem record of precipitation from the Yucatan Peninsula spanning the Maya Preclassic Period. *Global and Planetary Change* **138**, 93-102. https://doi.org/10.1016/j.gloplacha.2015.10.003

Medina-Elizalde, M., Polanco-Martínez, J. M., Lases-Hernández, F., Bradley, R., & Burns, S. (2016b). Testing the "tropical storm" hypothesis of Yucatan Peninsula climate variability during the Maya Terminal Classic Period. *Quaternary Research* **86**, 111–119. https://doi.org/10.1016/j.yqres.2016.05.006

Medina-Elizalde, M., Burns, S.J., Polanco-Martinez, J.M., Lases-Hernández, F., Bradley, R., Wang H. et al. (2017). Synchronous precipitation reduction in the American Tropics associated with Heinrich 2. *Scientific Reports* **7**, 11216. https://doi.org/10.1038/s41598-017-11742-8

Mestas-Nuñez, A. M., Enfield, D. B., & Zhang, C. (2007). Water vapor fluxes over the Intra-Americas Sea: Seasonal and interannual variability and associations with rainfall. *Journal of* Climate, **20**(9), 1910–1922. https://doi.org/10.1175/JCLI4096.1

Metcalfe, S., Breen, A., Murray, M., Furley, P., Fallick, A., & McKenzie, A. (2009). Environmental change in northern Belize since the latest Pleistocene. *Journal of Quaternary Science* **24**, 627–641. https://doi.org/10.1002/jqs.1248

Muñoz, E., Busalacchi, A. J., Nigam, S., & Ruiz-Barradas, A. (2008). Winter and summer structure of the Caribbean low-level jet. *Journal of Climate*, **21**(6), 1260–1276. https://doi.org/10.1175/2007JCLI1855.1

Pausata, F. S. R., Emanuel, K. A., Chiacchio, M., Diro, G. T., Zhang, Q., Sushama, L., et al. (2017). Tropical cyclone activity enhanced by Sahara greening and reduced dust emissions during the African Humid Period. *Proceedings of the National Academy of Sciences of the United States of America*, *114*(24), 6221–6226. https://doi.org/10.1073/pnas.1619111114

Pollock, A. L., van Beynen, P. E., DeLong, K. L., Asmerom, Y., & Reeder, P. P. (2016). A mid-Holocene paleoprecipitation record from Belize. *Palaeogeography Palaeoclimatology Palaeoecology* **463**, 103–111. https://doi.org/10.1016/j.palaeo.2016.09.021

Roberts, M. S., Smart, P. L., & Baker, A. (1998). Annual trace element variations in a Holocene speleothem. *Earth and Planetary Science Letters* **154**(1-4), 237-246 https://doi.org/10.1016/S0012-821X(97)00116-7

Rosenmeier, M. F., Hodell, D. A., Brenner, M., Curtis, J. H., & Guilderson, T. P. (2002). A 4000-year lacustrine record of environmental change in the southern Maya lowlands, Petén, Guatemala. *Quaternary Research*, **57**(2), 183–190. https://doi.org/10.1006/qres.2001.2305

Rowell, D. P., Folland, C. K., Maskell, K., Owen, J. A., & Ward, M. N. (1992). Modelling the influence of global sea surface temperatures on the variability and predictability of seasonal Sahel rainfall. *Geophysical Research Letters*, **19**(9), 905–908. https://doi.org/10.1029/92GL00939

Roy, P., Torrescano-Valle, N., Islebe, G., & Gutiérrez-Ayala, L. V. (2017). Late Holocene hydroclimate of the western Yucatan Peninsula (Mexico). *Journal of Quaternary Science* **32**(8), 1112-1120. https://doi.org/10.1002/jqs.2988

Sinclair, D. J., Banner, J. L., Taylor, F. W., Partin, J., Jenson, J., Mylroie, J. et al. (2012). Magnesium and strontium systematics in tropical speleothems from the Western Pacific. *Chemical Geology* **294-295**, 1-17. https://doi.org/10.1016/j.chemgeo.2011.10.008

Stahle, D. W., Burnette, D. J., & Diaz, J.V. (2012). Pacific and Atlantic influences on Mesoamerican climate over the past millennium. *Climate Dynamics* **39**(6), 1431-1446. https://doi.org/10.1007/s00382-011-1205-z

Sutton, R. T., & Hodson, D. L. R. (2005). Ocean science: Atlantic Ocean forcing of North American and European summer climate. *Science*, **309**(5731), 115–118. https://doi.org/10.1126/science.1109496

Tremaine, D. M., Froelich, P. N., & Wang, Y. (2011). Speleothem calcite farmed in situ: Modern calibration of $\delta^{18}O$ and $\delta^{13}C$ paleoclimate proxies in a continuously-monitored natural cave system. *Geochimica et Cosmochimica Acta* **75**(17), 4929-4950. https://doi.org/10.1016/j.gca.2011.06.005

Tremaine, D. M., & Froelich, P. N. (2013). Speleothem trace element signatures: A hydrologic geochemical study of modern cave dripwaters and farmed calcite. *Geochimica et Cosmochimica Acta* **121**, 522-545. https://doi.org/10.1016/j.gca.2013.07.026

Vuille, M., Bradley, R. S., Healy, R., Werner, M., Hardy, D. R., Thompson, L. G., & Keimig, F. (2003). Modeling δ18O in precipitation over the tropical Americas: 2. Simulation of the stable isotope signal in Andean ice cores. *Journal of Geophysical Research D: Atmospheres*, **108**(6). https://doi.org/10.1029/2001jd002039

Whitmore, T. J., Brenner, M., Curtis, J. H., Dahlin, B. H., & Leyden, B. W. (1996). Holocene climatic and human influences on lakes of the Yucatan Peninsula, Mexico: An interdisciplinary, palaeolimnological approach. *Holocene*, *6*(3), 273–287. https://doi.org/10.1177/095968369600600303

Willmott, C. J., & K. Matsuura (2001). Terrestrial Air Temperature and Precipitation: Monthly and Annual Time Series (1950 - 1999), http://climate.geog.udel.edu/~climate/html_pages/README.ghcn_ts2.html

Wong, C. I., & Breecker, D. O. (2015). Advancements in the use of speleothems as climate archives. *Quaternary Science Reviews* **127**, 1-18. https://doi.org/10.1016/j.quascirev.2015.07.019

Guoxiong Wu, & Ngar-Cheung Lau. (1992). A GCM simulation of the relationship between tropical-storm formation and ENSO. *Monthly Weather Review*, **120(6)**, 958–977. https://doi.org/10.1175/1520-0493(1993)121<2137:cogsot>2.0.co;2